

Research Update: Comparison of salt- and molecular-based iodine treatments of PbS nanocrystal solids for solar cells

Journal Article**Author(s):**

Jähmig, Fabian; Bozyigit, Deniz; [Yarema, Olesya](#) ; [Wood, Vanessa](#) 

Publication date:

2015-02-03

Permanent link:

<https://doi.org/https://doi.org/10.3929/ethz-b-000112628>

Rights / license:

[Creative Commons Attribution 3.0 Unported](#)


Originally published in:

APL Materials 3(2), <https://doi.org/10.1063/1.4907158>

Research Update: Comparison of salt- and molecular-based iodine treatments of PbS nanocrystal solids for solar cells

Cite as: APL Mater. 3, 020701 (2015); <https://doi.org/10.1063/1.4907158>

Submitted: 15 December 2014 . Accepted: 20 January 2015 . Published Online: 03 February 2015

Fabian Jähnig, Deniz Bozyigit , Olesya Yarema, and Vanessa Wood



View Online



Export Citation



CrossMark

ARTICLES YOU MAY BE INTERESTED IN

[Inorganic-ligand exchanging time effect in PbS quantum dot solar cell](#)

Applied Physics Letters **109**, 063901 (2016); <https://doi.org/10.1063/1.4960645>

[Single-step colloidal quantum dot films for infrared solar harvesting](#)

Applied Physics Letters **109**, 183105 (2016); <https://doi.org/10.1063/1.4966217>

[Charge dynamics at heterojunctions for PbS/ZnO colloidal quantum dot solar cells probed with time-resolved surface photovoltage spectroscopy](#)

Applied Physics Letters **108**, 091603 (2016); <https://doi.org/10.1063/1.4943077>



Top 5 Most Common Errors
in Magnetic Measurement

Download whitepaper 

Research Update: Comparison of salt- and molecular-based iodine treatments of PbS nanocrystal solids for solar cells

Fabian Jähnig, Deniz Bozyigit, Olesya Yarema, and Vanessa Wood
Laboratory for Nanoelectronics, ETH Zurich Gloriastrasse 35, Zurich 8044, Switzerland

(Received 15 December 2014; accepted 20 January 2015; published online 3 February 2015)

Molecular- and salt-based chemical treatments are believed to passivate electronic trap states in nanocrystal-based semiconductors, which are considered promising for solar cells but suffer from high carrier recombination. Here, we compare the chemical, optical, and electronic properties of PbS nanocrystal-based solids treated with molecular iodine and tetrabutylammonium iodide. Surprisingly, both treatments increase—rather than decrease—the number density of trap states; however, the increase does not directly influence solar cell performance. We explain the origins of the observed impact on solar cell performance and the potential in using different chemical treatments to tune charge carrier dynamics in nanocrystal-solids. © 2015 Author(s). All article content, except where otherwise noted, is licensed under a Creative Commons Attribution 3.0 Unported License. [<http://dx.doi.org/10.1063/1.4907158>]

Due to their excellent optical properties and ability to be solution processed into semiconducting thin films, colloiddally synthesized nanocrystals (NCs) are promising materials for the fabrication of low-cost and high performance optoelectronic devices such as solar cells.¹ However, because of their non-stoichiometric surface chemistry and high surface-to-volume ratio, thin films fabricated from NCs can exhibit electronic trap states within the band gap, which are believed to act as recombination centers.^{2,3}

Different chemical treatments have been applied with the goal of passivating trap states and have shown enhanced device performance.²⁻⁴ Early treatments used organic molecules to link the NCs while simultaneously passivating trap states.⁵⁻⁷ Treatments to assembled NC solids with tetrabutylammonium (TBA)-salts have been used to introduce halides, which bind to the surface of the NCs,^{2,4,8-11} and have yielded the highest power conversion efficiency (PCE) devices.⁴ Recently, a new kind of treatment utilizing halogens showed improved optical properties of PbSe NCs.¹² Molecular chlorine (Cl₂), added to a solution of NCs, etches away surface sulfur ions replacing them with Cl, creating a sub-monolayer thick shell around the NC, which is believed to shield PbSe and PbS NCs against oxidation.¹²

Here, we investigate the differences in molecular and salt-based passivation of NC solids, their influence on trap states' densities, and their impact on solar cell performance. Since the salt tetrabutylammonium iodide (TBAI) was successfully used to improve solar cell performance,⁴ we first demonstrate a method for molecular iodine (I₂) treatment and then compare different treatments containing iodide (I⁻) or iodine (I₂).

We fabricate and characterize metal-semiconductor-metal (MSM) diodes with four different lead sulfide (PbS) NC-based active layers (see Figure 1(a)): a reference (“REF”), two with salt-based treatments (“I⁻” and “I⁻-rinsed”), and one with a molecular treatment (I₂). We use PbS NCs,¹³ since they are the most studied material for solar cell applications. The synthesis conditions for our NCs and transmission electron microscope (TEM) images, showing an average NC diameter of 4 nm, are found in supplementary material Figure S1.¹⁴ The MSM diode structure^{5,15-17} is selected to minimize the number of materials and interfaces. For all devices, a NC-solid is formed on a patterned, transparent indium tin oxide (ITO) electrode by layer-by-layer deposition. The ITO-coated glass substrate is sequentially dipped into a NC solution (concentration 6 mg/ml in hexane), a 6 mM 1,2-ethanedithiol (EDT) in acetonitrile (ACN) solution, and ACN as a rinsing step. These dipcoating steps are repeated

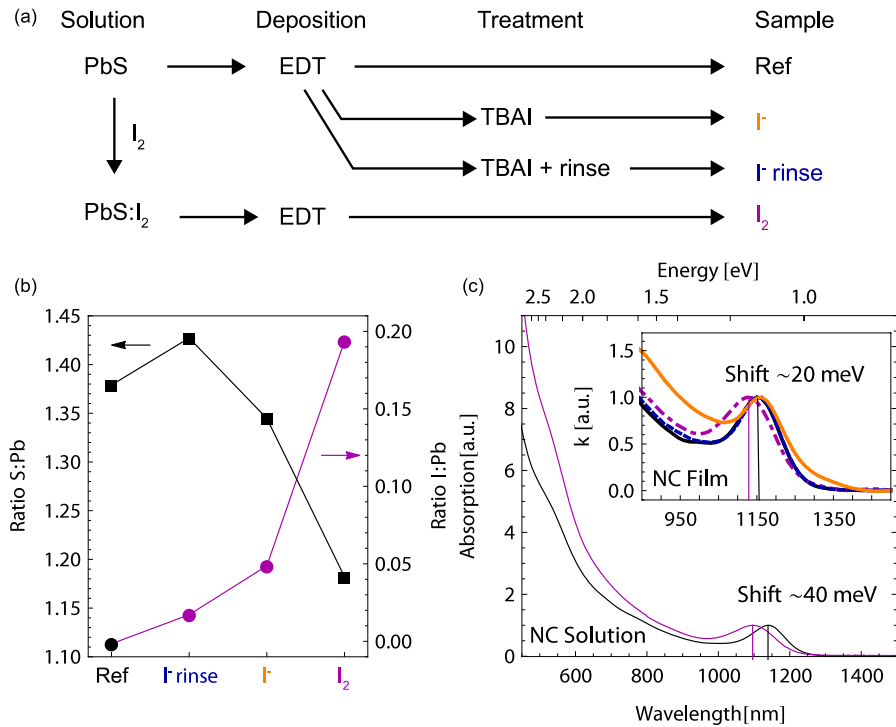


FIG. 1. (a) Scheme showing preparation steps for each of the four types of devices: reference, I⁻, I⁻ rinse, and I₂. (b) ICP-OES data showing ratios of I to Pb (black squares) and S to Pb (purple circles) in the four types of devices. (c) Solution absorption data for the as-synthesized (black) and I₂-treated (purple) NCs normalized to the first exciton absorption. Inset shows absorption near the first exciton peak from thin films: reference (black), I⁻ (blue), I⁻ rinse (orange), and I₂ (purple).

until a film thickness of 100 nm is reached (see supplementary material¹⁴ Figure S2). The top electrode consists of 1.5 nm lithium fluoride (LiF), 100 nm of aluminum, and 200 nm of silver deposited via thermal evaporation. The process describes the REF device.

The molecular iodine (I₂) treatment is performed on the PbS NCs in solution. First, a known amount of solid iodine is dissolved in hexane to achieve a solution with a 8.25 mM concentration. Then, 5.78 ml of this solution is added to 4.0 ml solution of PbS NCs dispersed in hexane at a concentration of 21 mg/ml. This mixture is stirred for 5 min. Subsequently, precipitation via ethanol, centrifugation, and re-dispersion in hexane is carried out to remove any excess I₂ and quench the reaction. Concentrations for iodine solution and the length of exposure time are selected through a series of experiments where the position of the exciton transition is monitored as a function of the different parameters. High concentrations of iodine were found to dissolve the NCs in agreement with Ref. 12. The above treatment procedure is optimized to shift the exciton peak of the NC solution to slightly higher energies (~40 meV) while still making it possible to keep the NCs dispersed in solution. Analyzing TEM pictures of the PbS NCs before and after (supplementary material Figure S1)¹⁴ the I₂ treatment shows that the NCs slightly increase in size from 3.54 ± 0.37 nm to 4.25 ± 0.50 nm consistent with the growth of a PbI₂ shell.

The treatment with the TBAI salt is performed on the assembled PbS NC-solid prior to deposition of the LiF/Al electrode. The NC film on ITO is soaked for 1 min in a TBAI salt dissolved in acetonitrile with a concentration of 10 mg/ml. Afterwards, excess solution is removed using a spincoater. For one sample (“I⁻ rinsed”), the PbS NC film is rinsed with acetonitrile following the treatment step. For another sample (“I⁻”), no rinsing is carried out.

Prior to measuring the solar cell characteristics of our devices, we quantify the effect of our treatments on the chemical composition of the films, their optical properties, and the electronic trap states in the band gap. To measure the effects of the treatments on chemical composition of the films, we use inductively coupled plasma optical emission spectrometry (ICP-OES) to determine

the amount of Pb, S, and I contained in each film. To obtain reliable and reproducible measurements with iodine, we dissolve our films in a basic medium (40% KOH). Figure 1(b) shows the ratios of iodine to lead (I:Pb) and sulfur to lead (S:Pb) for the different treatment methods. For both TBAI treatments, we observe a I:Pb ratio of about 4.5% for the I^- treated device and 1.3% for the I^- rinsed device. This suggests that I^- stays on the surface of the film during the treatment, which can be rinsed off and only a fraction diffuses into it. This is consistent with infrared absorption measurements shown in supplementary material Figure S3.¹⁴ In comparison, the I_2 treatment results in a 20% iodine to lead ratio (I:Pb). The S:Pb ratio of the reference film is 1.4 due to the additional sulfur atoms provided by the two thiolate groups of the EDT linker molecules. For the I_2 treatment, we see that the S:Pb ratio decreases by the same amount as the I:Pb ratio increases (20%). This indicates that I^- ions occupy and block positions, which would otherwise be occupied by thiolate groups (S^- -R) from the EDT crosslinker.

Absorption measurements of the reference NCs and the I_2 treated NCs in solution (see Figure 1(c)) show a blueshift of the exciton peak in the absorption spectrum by about 40 meV for the I_2 treated dots. The shift to higher energies as well as the increase in absorption in the visible indicates the formation of a PbI_2 shell during the I_2 treatment, consistent with increased NC size witnessed in the TEM images of the NCs in supplementary material Figures S1(a) and S1(b).¹⁴ Due to the larger band gap of bulk PbI_2 (2.5 eV) compared to PbS (0.41 eV),^{18,19} the exciton in the NC is more strongly confined and shifts to a higher energy. Using the shift in the exciton peak position, we estimate that the growth of the “shell” reduces the effective core size by 0.2 nm.²⁰

The inset of Figure 1(c) shows the normalized absorption around the first excitonic transition around 1.1 eV of NC thin films taken from ellipsometric data measured of films deposited on Si substrates, as explained in supplementary material.¹⁴ Exciton peaks are shifted to the red (lower energies) compared to the position found in solution, but the I_2 treated film is again shifted to slightly higher energies (+20 meV) as has been seen in the absorption data in solution. In contrast, the peak position does not shift for the TBAI treatments indicating that the energetic confinement of the electrons in the NCs is not modified by this treatment.

We also apply thermal admittance spectroscopy (TAS) on the REF, I_2 , and I^- NC-solids to quantify the energy and density of trap states (Figure 2). TAS is an electronic spectroscopy that measures the diode capacitance (C) in the dark at different temperatures (T) and frequencies (ω) to reconstruct the density and energy of trap states.^{21,22} For the reference sample (Figure 2(a)), we use the density-plot of $\omega dC/d\omega$ to extract a trap activation energy (E_T) of 155 meV and a reduced attempt frequency of (ν_{00}) of $6.4 \times 10^3 \text{ s}^{-1}\text{K}^{-2}$. Plotting the values of $\omega dC/d\omega$ along the line fitted on the density plot versus inverse temperature, we obtain a trap detuning energy (E_{TF}) of 7 meV and a trap density (N_T) of $3.1 \times 10^{16} \text{ cm}^{-3}$. We refer to this trap state as T1 in analogy to a similar discrete trap state, which we have previously observed by deep-level transient spectroscopy (DLTS), TAS, and Fourier-transform photocurrent spectroscopy (FTPS) in PbS -NC solids.²³ We perform the same measurement and analysis for the other devices (Figures 2(b)-2(d)) and tabulate the parameters in Figure 2(e). All activation energies (E_T) for the T1 trap state are similar and in the range of 100-160 meV, independent of the type of treatment that was applied. In TAS measurements, only trap states close to the Fermi-energy are visible; therefore, E_T is a good measure of the Fermi-energy at the trap position. The fact that E_T is similar in all samples indicates that the Fermi-energy in the material is determined by factors in common by all samples: dipcoating solutions (EDT/ACN) and electrodes (ITO, LiF/Al/Ag). The T1 trap state is present in the I^- samples and is increased in density by over a factor of 10 compared to the REF sample. The I_2 sample shows the presence of a second discrete trap state (T2) with a density of $5.85 \times 10^{18} \text{ cm}^{-3}$ and lower attempt frequency ($1.8 \text{ s}^{-1}\text{K}^{-2}$ vs. $1.0 \times 10^4 \text{ s}^{-1}\text{K}^{-2}$).

Figure 3 shows current-voltage (IV) measurements of the four types of devices in the dark and under AM1.5G illumination. Each curve is an average of measurements from eight devices. Comparing the dark currents (Figure 3(a)), we observe that (1) sweeping from forward ($V > 0$) to reverse ($V < 0$) bias, the dark current of the I^- device has a significantly larger hysteresis and reverse current than all other devices (REF, I^- rinse, and I_2) and (2) the series resistance for the I_2 device is 5-times larger than in the other devices. Two aspects pertaining to the solar cell performance (Figure 3(b)) are also immediately clear: (1) the open circuit voltage (V_{oc}) is increased for the I_2 device and (2) the

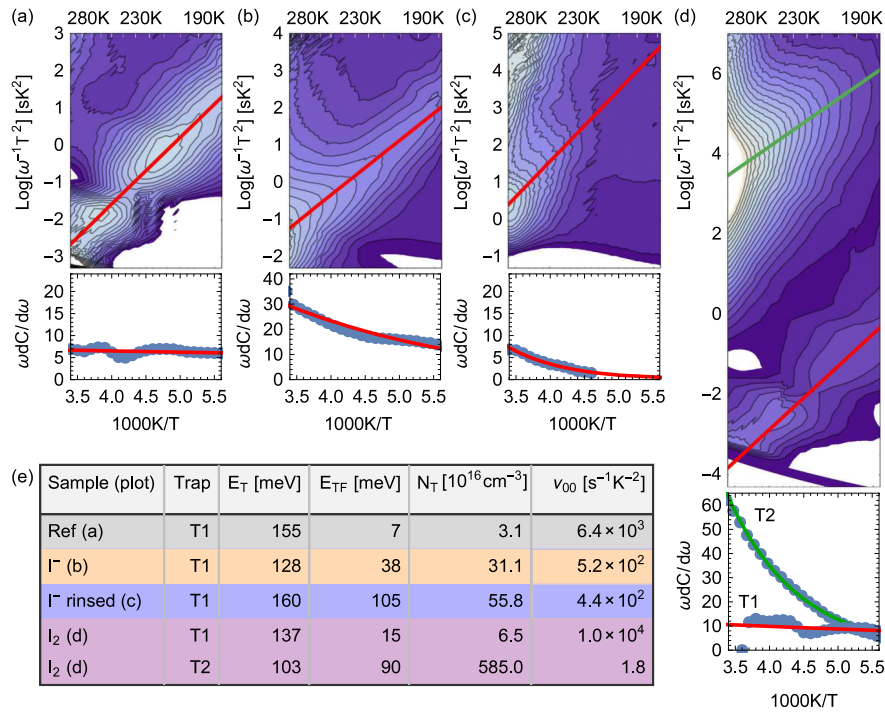


FIG. 2. TAS data from 180 K to 295 K for the samples: reference (a), I^- (b), I^- rinse (c), and I_2 treated (d). The density-plot (top) shows the derivative of the measured capacitance ($\omega dC/d\omega$). A linear fit gives the trap state activation energy (E_T) and the reduced attempt frequency (ν_{00}). The plot below shows $\omega dC/d\omega$ along the line in the density-plot above with a fit of the Fermi-Dirac-distribution, which allows determination of the detuning energy (E_{TF}) and the trap state density (N_T). To determine N_T , we account for E_{TF} .²² All parameters are tabulated in the table in (e).

short circuit current (J_{sc}) decreases for both the I^- and I_2 devices. The reference device displays an open-circuit voltage of $V_{oc} = 0.35$ V, a short-circuit current of $J_{sc} = 11.58 \pm 0.65$ mA/cm², and a power conversion efficiency of $\eta = 1.93\% \pm 0.11\%$. If the film is not rinsed after the I^- treatment, no working solar cell can be obtained (orange, dashed). In contrast, the device that was rinsed after the I^- treatment shows an open-circuit voltage $V_{oc} = 0.353 \pm 0.003$ V, similar to the reference sample, while it shows a reduction in current by about 25% to $J_{sc} = 8.64 \pm 0.55$ mA/cm². The I_2 device exhibits an even larger (54%) decrease in current compared to the reference to $J_{sc} = 5.34 \pm 0.88$ mA/cm² but a significant increase in open circuit voltage to $V_{oc} = 0.438 \pm 0.018$ V.

Bringing together our findings from the chemical, optical, and electronic characterizations of our treatments and their effects on device performance, we identify some characteristics of the salt and molecular based treatments. The large hysteresis in the dark IV curve for the I^- treatment, which is reduced after the rinsing step (I^- rinse), indicates the presence of an ionic species, which can move slowly in the film and change the electric potential for the free charge carriers. The rinsing step reduces this hysteresis suggesting that the ionic species can be washed out by acetonitrile and is supported by the observation that the amount of iodine in the sample is also reduced. The short circuit current J_{sc} is dictated by the built-in field and the selectivity of the electrodes.²⁴ We, therefore, expect J_{sc} to be altered by the presence of mobile ions. Indeed, we observe that J_{sc} is strongly reduced in the I^- sample and recovers after the rinsing.

In contrast to the I^- devices, the I_2 devices have no significant hysteresis but a 5-fold increase in the series resistance (R_s). We have recently shown that the series resistance is determined by the mobility (μ) of the NC-solid ($R_s \propto \mu$), which is very sensitive to tunnel barrier height and width between NCs.^{25,26} Our previous observations of substitution of S by I (Figure 1(b)) and the increase in the exciton energy (Figure 1(c) inset) indicate that the I_2 treatment forms a thin wider band gap PbI_2 shell on the NCs. This shell acts as a barrier for charge carriers and is consistent with the 5-fold reduction of the mobility.

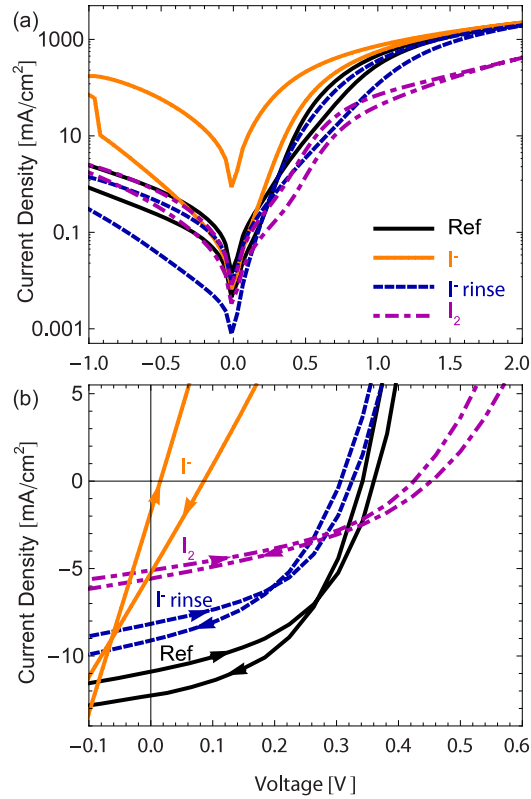


FIG. 3. Current density vs. voltage characteristics of the reference (black), I^- (blue), I^- rinse (orange), and I_2 treated (purple) (a) in the dark and (b) under AM1.5G illumination with arrows indicating the direction of the voltage sweep. The I^- treated device without a rinse shows a distinct hysteresis. With respect to the reference EDT device, the short circuit current (J_{sc}) decreases for devices with the I^- and I_2 treatments while the V_{oc} increases for the I_2 treated device.

The reduction in mobility in the I_2 device further explains the 80 mV increase of the open-circuit voltage (V_{oc}) compared to the REF device. The limit of the V_{oc} is given by²⁵

$$eV_{oc} = E_{\mu} + n_{id} kT (\log(J_{sc}) - \log(J_0 T^2)), \quad (1)$$

where E_{μ} is the mobility band gap, n_{id} the ideality factor, J_0 the reduced saturation current of the diode, and kT the thermal energy. Since E_{μ} is given by the optical exciton energy,²⁵ it increases by 20 meV (Figure 1(c) inset) between the REF device and the I_2 device. The second term ($n_{id} kT \log(J_{sc})$) in Eq. (1) leads to a decrease of -43 meV due to the lower J_{sc} (43%) for an ideality factor if $n_{id} = 2$. To achieve the observed +80 mV increase in V_{oc} , the last term ($-n_{id} kT \log(J_0 T^2)$) must therefore increase by 103 meV, which corresponds to a 7-fold decrease in J_0 . Details on the arguments with respect to the choice of units in Eq. (1) are found in the supplementary material.¹⁴ This decrease can be understood in the following way: The dark current in NC-diodes results from trap-assisted recombination of electrons and holes and this recombination is controlled by diffusion,²⁵ in agreement with previous reports,^{27,28} and therefore the saturation current is proportional to the charge carrier mobility ($J_0 \propto \mu$). The decrease in J_0 originates from the same decrease in mobility that causes the increase in the series resistance.

Surprisingly, the large increases in trap state density (N_T) determined by TAS (Figure 2) do not show a clear effect on the behavior and performance of the I^- rinsed and the I_2 treated diodes. In particular, comparing the V_{oc} of the I^- rinse and I_2 devices to the REF device, we see that the V_{oc} are similar or even higher, which suggests a similar number of active recombination centers. We interpret this by noting that the observed T1 and T2 trap states are not the dominant recombination centers in the device, consistent with the fact that they are far away from the middle of the bandgap (100-160 meV below the conduction band). In agreement with our previous findings, we conclude

that the observed trap states influence device behavior by changing of the Fermi-level in the device, rather than by mediating recombination.^{23,25}

In summary, we have explored two routes for iodine passivation in PbS NC-solar cells using Γ -ions (TBAD) and molecular I_2 . The Γ -treatment does not bind iodine in a stable fashion in the NC-solid, and we observe the movement of ions as a large hysteresis in the device. The I_2 treatment leads to the formation of a thin PbI_2 shell, which we observe by increased confinement (+20 meV) and reduced mobility (~5-7 fold). The reduced mobility leads to a higher series resistance, lower J_{sc} , but higher V_{oc} , which is in agreement with our previous findings.²⁵ Both treatments show a clear increase of the density of trap states as determined by TAS, which is not reflected in the current-voltage characteristics of the device. This suggests that performance improvements observed after halogen treatments might not result from the elimination of recombination centers,^{2,3} but rather from other charge carrier physics such as the modification of energetic barriers by surface dipoles.^{4,8}

The authors thank David Norris for use of ICP-OES and Ian Rousseau for assistance with the ellipsometry measurements. The authors acknowledge support of the Scientific Center for Optical and Electron Microscopy ScopeM of the Swiss Federal Institute of Technology ETHZ for the use of the TEM. Project funding is from the Swiss National Science Foundation for the Quantum Science and Technology NCCR and an independent research grant.

- ¹ I. J. Kramer and E. H. Sargent, *Chem. Rev.* **114**, 863 (2014).
- ² J. Tang, K. W. Kemp, S. Hoogland, K. S. Jeong, H. Liu, L. Levina, X. Wang, R. Debnath, D. Cha, K. W. Chou, A. F. Aram, J. B. Asbury, E. H. Sargent, M. Furukawa, A. Fischer, and A. Amassian, *Nat. Mater.* **10**, 765 (2011).
- ³ A. H. Ip, S. M. Thon, S. Hoogland, O. Voznyy, D. Zhitomirsky, R. Debnath, L. Levina, L. R. Rollny, G. H. Carey, A. Fischer, K. W. Kemp, I. J. Kramer, Z. Ning, A. J. Labelle, K. W. Chou, A. Amassian, and E. H. Sargent, *Nat. Nanotechnol.* **7**, 577 (2012).
- ⁴ C.-H. M. Chuang, P. R. Brown, V. Bulović, and M. G. Bawendi, *Nat. Mater.* **13**, 796 (2014).
- ⁵ J. P. Clifford, K. W. Johnston, L. Levina, and E. H. Sargent, *Appl. Phys. Lett.* **91**, 253117 (2007).
- ⁶ J. M. Luther, M. Law, Q. Song, C. L. Perkins, M. C. Beard, and A. J. Nozik, *ACS Nano* **2**, 271 (2008).
- ⁷ G. I. Koleilat, L. Levina, H. Shukla, S. H. Myrskog, S. Hinds, A. G. Pattantyus-Abraham, and E. H. Sargent, *ACS Nano* **2**, 833 (2008).
- ⁸ P. R. Brown, D. Kim, R. R. Lunt, N. Zhao, M. G. Bawendi, J. C. Grossman, and V. Bulović, *ACS Nano* **8**, 5863 (2014).
- ⁹ Z. Ning, Y. Ren, S. Hoogland, O. Voznyy, L. Levina, P. Stadler, X. Lan, E. H. Sargent, and D. Zhitomirsky, *Adv. Mater.* **24**, 6295 (2012).
- ¹⁰ D. Zhitomirsky, M. Furukawa, J. Tang, P. Stadler, S. Hoogland, O. Voznyy, H. Liu, and E. H. Sargent, *Adv. Mater.* **24**, 6181 (2012).
- ¹¹ S. Kim, J. Noh, H. Choi, H. Ha, J. H. Song, H. C. Shim, J. Jang, M. C. Beard, and S. Jeong, *J. Phys. Chem. Lett.* **5**, 4002 (2014).
- ¹² W. K. Bae, J. Joo, L. A. Padilha, J. Won, D. C. Lee, Q. Lin, W.-K. Koh, H. Luo, V. I. Klimov, and J. M. Pietryga, *J. Am. Chem. Soc.* **134**, 20160 (2012).
- ¹³ M. A. Hines and G. D. Scholes, *Adv. Mater.* **15**, 1844 (2003).
- ¹⁴ See supplementary material at <http://dx.doi.org/10.1063/1.4907158> for material synthesis and characterization, Figure S1; film characterization, Figure S2; fitting of ellipsometry data; ligand exchange and infrared absorption, Figure S3; and details on the assessment of the change in open-circuit voltage.
- ¹⁵ K. Szendrei, W. Gomulya, M. Yarema, W. Heiss, and M. A. Loi, *Appl. Phys. Lett.* **97**, 203501 (2010).
- ¹⁶ J. Tang, X. Wang, L. Brzozowski, D. A. R. Barkhouse, R. Debnath, L. Levina, and E. H. Sargent, *Adv. Mater.* **22**, 1398 (2010).
- ¹⁷ D. Bozyigit and V. Wood, *J. Mater. Chem. C* **2**, 3172 (2014).
- ¹⁸ C. Gähwiller and G. Harbeke, *Phys. Rev.* **185**, 1141 (1969).
- ¹⁹ W. W. Scanlon, *J. Phys. Chem. Solids* **8**, 423 (1959).
- ²⁰ L. Cademartiri, E. Montanari, G. Calestani, A. Migliori, A. Guagliardi, and G. A. Ozin, *J. Am. Chem. Soc.* **128**, 10337 (2006).
- ²¹ T. Walter, R. Herberholz, C. Müller, and H. W. Schock, *J. Appl. Phys.* **80**, 4411 (1996).
- ²² D. Bozyigit and V. Wood, preprint [arXiv: 1412.4087](https://arxiv.org/abs/1412.4087) (2014).
- ²³ D. Bozyigit, S. Volk, O. Yarema, and V. Wood, *Nano Lett.* **13**, 5284 (2013).
- ²⁴ I. Mora-Sero, L. Bertoluzzi, V. Gonzalez-Pedro, S. Gimenez, F. Fabregat-Santiago, K. W. Kemp, E. H. Sargent, and J. Bisquert, *Nat. Commun.* **4**, 2272 (2013).
- ²⁵ D. Bozyigit, W. M. Lin, N. Yazdani, O. Yarema, and V. Wood, *Nat. Commun.* **6**, 6180 (2015).
- ²⁶ A. Shabaev, A. L. Efros, and A. L. Efros, *Nano Lett.* **13**, 5454 (2013).
- ²⁷ D. Zhitomirsky, O. Voznyy, L. Levina, S. Hoogland, K. W. Kemp, A. H. Ip, S. M. Thon, and E. H. Sargent, *Nat. Commun.* **5**, 3803 (2014).
- ²⁸ W. Yoon, J. E. Boercker, M. P. Lumb, D. Placencia, E. E. Foos, and J. G. Tischler, *Sci. Rep.* **3**, 2225 (2013).